Functional Modularity of the Arginine Catabolic Mobile Element Contributes to the Success of USA300 Methicillin-Resistant *Staphylococcus aureus*

Lance R. Thurlow, **Gauri S. Joshi**, **Justin, R. Clark**, **Jeffrey S. Spontak**, **Crystal J. Neely**, **Robert Maile**, and **Anthony R. Richardson**[*]
Department of Microbiology and Immunology The University of North Carolina at Chapel Hill Chapel Hill, NC 27599 USA

Summary

The successful USA300 Community-Associated Methicillin-Resistant *Staphylococcus aureus* (CA-MRSA) lineage predominantly causes skin and soft tissue infections (SSTIs) and is highly associated with carriage of the Arginine Catabolic Mobile Element (ACME). However, the contribution of ACME to USA300 fitness during SSTIs remains incompletely understood. We show that the constitutive ACME-encoded arginine-deiminase system (Arc) allows USA300 to thrive in acidic environments that mimic human skin. Consequently, ACME-Arc drives excessive production of host polyamines, compounds uniquely toxic to *S. aureus*. To mitigate this, ACME also encodes SpeG, a polyamine-resistance enzyme that is essential for combating excess host polyamines in a murine SSTI model. Inhibiting host polyamine production not only restored $\Delta speG$ persistence within infected wounds but also severely altered the host healing process, implying that polyamines play integral roles in coordinating the wound-healing response. Together, these data underscore the functional modularity of ACME and its contribution to the success of USA300 CA-MRSA.

Introduction

Infections caused by Methicillin-Resistant *Staphylococcus aureus* (MRSA) have plagued healthcare settings for years (DeLeo et al., 2010). In the last two decades however, MRSA isolates have shifted from being exclusively hospital associated (HAMRSA) to the most common cause of community associated (CA-MRSA) skin and soft tissue infections (SSTIs) (Talan et al., 2011). The dominant CA-MRSA clones in the US belong to the pulsed-field type USA300 (McDougal et al., 2003). USA300 can account for 98% of MRSA SSTIs presenting to emergency rooms and has spread into healthcare settings causing the majority of nosocomial infections (Popovich et al., 2008; Talan et al., 2011). The increased prevalence of USA300 disease is partially explained by the overproduction of toxins resulting in hypervirulence in animal models (Bubeck Wardenburg et al., 2007; Li et al., 2009; Montgomery et al., 2008). However, hypervirulence alone cannot account for the dominance of USA300 CA-MRSA (Thurlow et al., 2012). For instance, the rapid

[*]Corresponding Author Anthony R. Richardson, Ph.D. Department of Microbiology & Immunology 116 Manning Dr, MEJ 512, CB7290 Chapel Hill, NC 27599 Ph (919) 843-3654 Fx (919) 962-8103 anthony_richardson@med.unc.edu.

replacement of other CA-MRSA lineages (*e.g.* USA400) in North America by USA300 clones entailed highly efficient transmission, a trait that cannot be fully explained by hypervirulence. Currently, our understanding of the factors that contribute to the remarkable success of USA300 clones is incomplete.

USA300 pathogenicity requires the overexpression of major virulence factors common among all *S. aureus* including Agr-regulated toxins (Bubeck Wardenburg et al., 2007; Kobayashi et al., 2011; Li et al., 2010; Montgomery et al., 2010). The exact mechanism behind the overproduction of these virulence traits in USA300 clones is not clear, but it has recently been demonstrated that other non-USA300 lineages also exhibit toxin overproduction (*e.g.* USA500) (Li et al., 2010). Additionally, USA300 isolates produce the Panton-Valentine Leukotoxin (PVL), but the exact contribution of PVL to USA300 disease is still unclear (Bubeck Wardenburg et al., 2008; Kobayashi et al., 2011; Lipinska et al., 2011; Loffler et al., 2010). Finally, most USA300 *S. aureus* from North America harbor the Arginine Catabolic Mobile Element (ACME) (Diep et al., 2008; Reyes et al., 2009). In contrast, ACME is only found in a rare subset of MRSA clones from Northern Europe and Japan (Bartels et al., 2011; Ellington et al., 2008; Shore et al., 2011; Urushibara et al., 2012). However, USA300 ΔACME mutants have only modest virulence defects in rabbit endocarditis, and no measurable phenotypes in murine sepsis or SSTIs (Diep et al., 2008; Montgomery et al., 2009). Thus, it is still unclear how ACME and other USA300 features act together to contribute to the emergence of epidemic CA-MRSA in North America.

SSTIs are the most common clinical presentations associated with USA300 CAMRSA disease (DeLeo et al., 2010; Talan et al., 2011). The surface of the skin is a harsh acidic environment given the low pH of sweat and scarce nutrients (Di Meglio et al., 2011). Furthermore, the epidermis is immunologically active and serves as a formidable barrier to invading pathogens. The dermal layer also hosts a variety of immune cells which respond robustly to cytokines, chemokines and available nutrients (Miller and Cho, 2011). Arginine is a prominent nutrient mediator in the cutaneous immune response as it is involved in both initial inflammation and subsequent resolution. Initially, infected tissue is inflamed and marked by cytokines such as IL-1, INF-γ and TNF-α with host arginine being primarily consumed by iNOS to generate nitric oxide (NO·) (Gantwerker and Hom, 2012; Satriano, 2004). Once signals from damaged tissue outweigh inflammatory cues, the host response shifts towards the synthesis of anti-inflammatory cytokines including IL-4, IL-10, IL-13 and TGF-β (Gantwerker and Hom, 2012). During this resolution phase, Arginase-1 (ARG-1) redirects arginine towards the production of ornithine (Satriano, 2004), which can be converted to a group of compounds collectively referred to as polyamines (*i.e.* putrescine (Put), spermidine (Spd) and spermine (Spd)) (Cohen, 2000).

Polyamines are critical for proper wound healing as they are anti-inflammatory and promote cell proliferation and tissue regeneration (Cohen, 2000; Curran et al., 2006). Polyamines were thought to be ubiquitous among all living organisms, however *S. aureus* lacks polyamine synthesis and is rapidly killed by physiological Spm concentrations (Joshi et al., 2011). The only exceptions to *S. aureus* polyamine-sensitivity were USA300 isolates (*e.g.* LAC and SF8300), which express an ACME-encoded Spm/Spd acetyltransferase (SpeG) that accounts for full polyamine-resistance. Thus, polyamine resistance is a unique characteristic that distinguishes USA300 from other *S. aureus*. However, whether SpeG contributes to virulence and/or persistence of USA300 *S. aureus* has never been established.

Here we demonstrate that the modular ACME island directly contributes to persistence in environments mimicking conditions found on human skin and within cutaneous abscesses. The constitutive arginine deiminase system (Arc) encoded on ACME allows USA300 to thrive in acidic environments similar to that of human sweat. However, once USA300 *S.*

aureus penetrates the epidermis, ACME-Arc drives excessive host polyamine synthesis necessitating SpeG. Thus, the acquisition of ACME allows USA300 to combat the high levels organic acids and polyamines in skin thereby contributing to the dominance of USA300 in SSTIs.

Results

Constitutive USA300 ACME Arc promotes survival in acidic environments

The pH of skin is low (~5.0) given the high abundance of lactic acid in sweat (Harvey et al., 2010). It has been proposed that ammonia produced by the ACME-encoded arginine deiminase system (ACME-Arc) may contribute to acid tolerance during skin colonization (Figure 1A) (Diep et al., 2006). Cultivating USA300 in defined medium buffered at pH 5.0 containing physiological levels of arginine and lactic acid resulted in 2-log growth over 24 h (Figures 1B and S1). In contrast, isogenic ΔACME and ΔArc mutants exhibited no significant growth under these conditions. Additionally, all similarly cultured non-USA300 *S. aureus* strains were unable to grow in acidic media (Figures 1B and S1). All strains grew equally well in defined medium buffered at or above pH 6.0 (data not shown). A plasmid harboring the ACME Arc gene cluster conferred full acid tolerance to *S. aureus* strain Newman (Figure 1B). Thus, the presence of ACME-Arc is necessary and sufficient for growth in acidic skin-like environments. These results imply that the ACME-Arc system is expressed in aerated media, a condition known to repress the Arc system from the core genome of all *S. aureus* (Harvey et al., 2010; Makhlin et al., 2007). In contrast to chromosomal Arc, ACME-Arc was constitutively expressed regardless of the presence of glucose and/or oxygen (Figure 1C). Thus, USA300 clones thrive in lactic acid-rich environments given the ammonia production derived from constitutive ACME-Arc expression.

S. aureus resists host inflammation but is effectively cleared within post-inflammatory abscesses

Host arginine feeds multiple pathways during a typical immune response (Figure 2A). Initially, infected tissue is inflamed and macrophages primarily consume arginine via iNOS to generate NO· (Gantwerker and Hom, 2012; Satriano, 2004). Over time, the host shifts away from NO· production and macrophages redirect arginine via ARG-1, towards the production of ornithine, which can be further converted to polyamines (Figure 2A) (Gantwerker and Hom, 2012; Satriano, 2004). In the murine SSTI model, subcutaneously injected USA300 *S. aureus* replicate and cause dermonecrotic lesions within 24 to 48 h (Figure 2B). Histological staining of *S. aureus* skin abscesses sections revealed high levels of infiltrating granulocytes surrounding central regions of necrosis (Figures 2D and S2). Infections typically resolve within two weeks as the contracting dermonecrotic lesion is encased within a fibrotic wall primarily composed of fibronectin and collagen. Immunohistological staining of *S. aureus* abscesses revealed an early inflammatory signature with high iNOS expression (Figure 2E). Eventually, the host response shifts to an anti-inflammatory phase with enhanced ARG-1 expression and little detectable iNOS (Figures 2E and 2F). The immunohistology was quantitatively validated using flow cytometry (Figure 2G). At day-7, abscesses possessed significant numbers of both ARG-1^{+} and iNOS[+] macrophages, but by day 12, abscesses were virtually devoid of iNOS^{+} cells and were highly enriched for Arg-1 (Figure 2G). Thus, only early abscesses are replete with NO·, an innate immune effector to which *S. aureus* is inherently resistant (Hochgrafe et al., 2008; Richardson et al., 2008). Accordingly, very little loss of bacterial viability is observed within the first week following *S. aureus* inoculation (Figure 2C). In contrast, NO·-sensitive *Staphylococcus epidermidis* and *Enterococcus faecalis* are rapidly cleared within inflamed abscesses underscoring their comparative sensitivity to inflammation. However, as the

healing process unfolds, *S. aureus* likely encounters less inflammation and is increasingly exposed to the post-inflammatory phase, which is notably efficient at clearing *S. aureus.* These data imply that the unique resistance of *S. aureus* to oxidative/nitrosative stresses enables persistence within early abscesses, but unidentified effectors expressed during the resolution phase exert potent anti-staphylococcal activity. Additionally, non-USA300 clones are particularly susceptible to this post-inflammatory killing mechanism in that MSSA strain Newman was significantly less viable than USA300 at day 12 (17-fold fewer viable cfu, p 0.01, Students t-test) (Figure 2C).

Host polyamines contribute to post-inflammatory clearing of *S. aureus*

SpeG-expressing USA300 clones are the only polyamine-resistant *S. aureus* strains known (Joshi et al., 2011). USA300 Δ*speG* begins to exhibit significantly less viability at day 7 when high-level ARG-1 expression is first observed (Figures 2F and 3A). By day 12, Δ*speG* is 23-fold less abundant than WT in healing abscesses (Figure 3A). Repairing the Δ*speG* allele fully restored WT persistence and *speG* was also required for full virulence in another USA300 background, LAC (Figure 3B). Moreover, abscesses were on average 6-fold larger in mice infected with WT LAC versus isogenic Δ*speG* (data not shown, p < 0.05, Mann-Whitney). Thus, SpeG-mediated polyamine-resistance provides a major fitness advantage to USA300 during SSTI. Staphylocidal polyamine levels steadily increase within *S. aureus* abscesses during the anti-inflammatory phase, peaking at day 12 (Figure 3C). To ascertain whether the Δ*speG* persistence defect resulted directly from host polyamines, we administered a potent inhibitor of ODC, difluoromethylornithine (DFMO, Figure 2A) (Sunkara and Rosenberger, 1987). DFMO-administration inhibited host synthesis of Spm and Spd (Figure 3C) and completely reversed the attenuation of Δ*speG* (Figure 3B). Not only did DFMO-treatment abolish the differences between WT and Δ*speG* viability, but abscesses in treated mice exhibited fifty-fold higher organism burdens compared to untreated animals. DFMO-treatment is known to alter the host immune response since intracellular polyamines can limit macrophage activation and iNOS expression (Baydoun and Morgan, 1998; Zhang et al., 2000). Thus, interfering with polyamine production leads to dysregulation of inflammation and wound healing. Indeed, by day 12 abscesses are normally highly structured, compact and surrounded by a meshwork of leukocytes and matrix proteins including collagen (Figures 3D and S2). In contrast, day 12 abscesses in DFMO treated mice are still highly disordered, lack typical ARG-1 or ODC signatures and exhibit robust iNOS expression with virtually no detectible collagen deposition.

Host polyamine production was also essential for controlling *S. aureus* sepsis in that DFMO treatment resulted in significantly higher mortality (Figure 4A). However, DFMO-treatment was detrimental to mice infected with both Spm-resistant USA300 as well as Spm-sensitive strain Newman. Moreover, isogenic polyamine-sensitive USA300 mutants (ΔACME and Δ*speG*) were not attenuated in a sepsis model (Figure 4B). These data imply that during sepsis, the anti-inflammatory aspects of polyamines are essential for controlling inflammation and tissue damage, however polyamines do not exert direct *S. aureus* killing. Consistent with this finding, infected organ tissue have significantly lower amounts of all three polyamine species when compared to infected skin (Figure 4C). Our data show that the benefit of ACME-encoded SpeG is particularly observable during skin infections where polyamine production is robust.

ACME-Arc drives excess host polyamine synthesis necessitating SpeG

The lack of ΔACME attenuation compared with that of Δ*speG* in SSTIs presents a paradox given that Δ*speG* and ΔACME are equally susceptible to polyamines (Figure S3A)(Joshi et al., 2011; Montgomery et al., 2009). We reasoned that ACME-Arc could divert tissue arginine from iNOS, toward polyamine production thereby necessitating SpeG (Figures 1A

and 2A). Accordingly, additional inactivation of the ACME-Arc system in the Δ*speG* background restored virulence, essentially phenocopying a ΔACME mutant (Figure S3A). Moreover, the presence of Arc in USA300 directly affected tissue polyamine levels. Day 12 abscesses that were significantly infected with ACME-Arc positive strains had ~50% more Put than abscesses infected with Arc-null mutants (Figure S3B). Furthermore, iNOS was less abundant in abscesses infected with Arc-positive USA300 (Figure S3C). This is consistent with lower tissue arginine levels in Arc-positive abscesses since iNOS expression is positively regulated by the availability of arginine (Chaturvedi et al., 2007). Collectively, these data show that ACME-Arc successfully competes with host iNOS for available arginine and subsequently drives excessive host polyamine synthesis thereby necessitating SpeG.

Discussion

Skin acidity stems from lactic acid in sweat and protonated organic acids can permeate bacterial membranes to exert intracellular acid stress (Gantwerker and Hom, 2012; Harvey et al., 2010). The ability to generate ammonia via the Arc system would greatly serve to balance intracellular pH in this environment (Figure 1A). However, the chromosomal Arc system of *S. aureus* is only active during anaerobic growth (Sun et al., 2012). The skin surface is sufficiently aerated, thus the core Arc system is not sufficient for surviving lactic acid stress (Figure 1B). In contrast, the ACME-Arc system is robustly expressed independently of glucose or oxygen and therefore provides acid tolerance in aerated environments. The mechanism by which constitutive ACME-Arc gene expression evolved is still unknown, but clearly, ACME-Arc provides an enormous advantage to USA300 when cultivated in an environment replete with organic acids abundant on human skin (Figure S1).

It has been further postulated that ACME-Arc may compete with iNOS for available arginine thereby limiting the amount of NO· produced in response to USA300 infection (Diep et al., 2006). Indeed, ACME-positive infections exhibited noticeably less iNOS staining at day 12 when compared to ACME-negative infections (Figure S3C). However, *S. aureus* is inherently resistant to NO· (Hochgrafe et al., 2008; Richardson et al., 2008) and iNOS-deficiency did not significantly affect the outcome of *S. aureus* SSTIs (Figure S4A). Even strains lacking the *S. aureus* flavohemoprotein (Δ*hmp*), which exhibit increased NO·-sensitivity were only modestly attenuated in the skin abscess model (Figure S4). Furthermore, combining the Δ*hmp* and Δ*arcA* (ACME) in USA300 did not result in synergistic attenuation implying that NO· is not abundant enough to drastically affect the outcome of *S. aureus* SSTI (Figure S4A). In contrast, iNOS has a dramatic effect on NO·-sensitive *S. epidermidis* during skin infection in that *S. epidermidis* could replicate to the same level as *S. aureus* in iNOS-deficient mice. Given that USA300 ACME was acquired from *S. epidermidis* (Diep et al., 2006; Goering et al., 2007; Miragaia et al., 2009), this island may have originally evolved to protect *S. epidermidis* from host NO·. However, *S. aureus* must maintain ACME for reasons other than allowing this intrinsically resistant organism to minimize NO·-exposure.

In the diseased state of a skin abscess, constitutive ACME-Arc drives host polyamine synthesis thereby necessitating SpeG-mediated polyamine detoxification (Figures S3 and 3). Polyamine synthesis is more robust in actively dividing cells (Cohen, 2000). The skin is an organ constantly undergoing regeneration and consequently, polyamine levels are reportedly higher in the lower strata of the epidermis than in most other organ sites (Baze et al., 1985). Moreover, during the wound-healing phase of a SSTI, multiple cell types are rapidly expanding creating a heightened polyamine requirement. Accordingly, polyamines are more than twice as abundant within day 12 abscesses than in resting skin (Figure 3C) and significantly more concentrated in healing skin than in infected internal organs (Figure 4C).

The generation of ornithine by strains expressing a constitutive ACME-Arc would provide for greater polyamine production in proliferating tissue (Figure 2A). Indeed, ACME-Arc expression results in a 50% increase in day 12 tissue Put when the abscess is still highly infected such that bacteria are numerous enough to exert measurable effects on host arginine metabolism (Figure S2B). Moreover, deletion of Δ*speG* alone significantly affected persistence, however eliminating ACME-Arc reverses the Δ*speG* phenotype (Figure S2A). This implies that the excess ornithine generated by constitutive ACME-Arc pushes polyamine levels to a point that requires SpeG-mediated detoxification. Taken together, these observations can explain the success of USA300 in the skin environment as it can persist in the presence of excess organic acids and polyamines. Accordingly, USA300 isolates are more commonly isolated from extranasal site than any other lineage (Miko et al., 2012; Schechter-Perkins et al., 2011).

Inhibiting *de novo* polyamine synthesis completely reversed the Δ*speG* phenotype (Figure 3B), despite the fact that DFMO treatment merely lowered Spm and Spd levels by ~50% (Figure 3C). The residual polyamine content of tissue from DFMO treated mice results from catabolism of dietary polyamines (Sunkara and Rosenberger, 1987). However, the observed drop in polyamine levels had drastic effects on *S. aureus* SSTI outcomes rendering the Δ*speG* mutant indistinguishable from WT USA300 (Figure 3B). Additionally, without *de novo* polyamine synthesis, the host response to *S. aureus* infection is significantly altered. DFMO treated mice exhibit no measurable fibrosis and wounds are still open, inflamed and highly infected at day 12 (Figures 3D, 3B and S1). Thus, not only do polyamines exert direct anti-staphylococcal effects during the resolution of SSTIs, but also they are essential for coordinating the host post-inflammatory healing response.

The contribution of ACME to virulence has been dismissed given the lack of virulence phenotypes associated with ΔACME strains (Montgomery et al., 2009). However, the functional modularity of ACME masks its direct role in USA300 persistence in the acidic skin environment and within healing abscesses. We contend that the success of USA300 stems from enhanced virulence factor production combined with increased fitness that accompanied the acquisition of the modular ACME island.

Materials and Methods

Bacterial Strains and Growth Conditions

Strains are listed in Table S1. Bacteria were grown in brain heart infusion (BHI), Tryptic soy Broth (TSB) or in chemically defined medium (PN) (Fuller, 2011) with or without 4 mM Arginine and 50 mM lactic acid buffered to pH 5.0. Growth was monitored by plating for viable cfu after 24 h of aerobic incubation at 37° C and comparing viable cfu to the inoculum (~1×10^6 cfu). Isogenic *S. aureus* Δ*arc* (ACME copy) mutants were constructed by amplifying ~1 kb 5′ and 3′ homology fragments using primers listed in Table S1. The resulting fragments were cloned on either side of the Sp^r cassette in the *E. coli*/*S. aureus* shuttle vector pBTSts (Table S1). SF8300 Δ*hmp* strains were constructed using pTR040 (Table S1). Allelic exchange was performed as previously described (Fuller, 2011).

Animal Studies

C57BL/6J mice and isogenic iNOS$^{-/-}$ mice were obtained from Jackson Labs (Bar Harbor, ME, USA). Subcutaneous infections were performed as previously described (Thurlow et al, 2011). Briefly, mice were anesthetized with 2,2-tribromoethanol, shaved, and injected with 20 μl of PBS containing 1×10^8 CFU of bacteria. DFMO was administered at 1% wt:vol in water one day prior to inoculation and continuing throughout infection. Mice were

euthanized and abscesses were collected to determine bacterial burdens and polyamine content on days 3, 7, and 12 post-inoculation.

For sepsis studies, mice were infected by tail vein injection with 5×10^6 CFU of bacteria. Mouse weights were monitored daily and mice were euthanized once 30% of their initial body weight was lost as per IACUC approved protocol.

Immunofluorescence staining

Immunohistochemistry on tissue was performed as previously described (Thurlow et al., 2011). Abscess tissue was fixed in 10% formalin, paraffin embedded, sectioned (10 μm), and H&E stained by the UNC Histopathology Core Facility. Unstained sections were deparaffinized using a graded series of xylene and ethanol washes followed by microwaving for 20 min in 10 mM sodium citrate buffer (pH 6) for antigen retrieval. Specimens were blocked in 10% donkey serum (Jackson ImmunoResearch, West Grove, PA, USA) and subsequently stained with antibodies specific for iNOS (Abcam, Cambridge, MA, USA), ARG-1 (Santa Cruz Biotechnology, Santa Cruz, CA, USA), Type 1 Collagen (Abcam), or ODC (US Biological, Swampscott, MA USA). Staining was detected using biotinylated secondary antibodies followed by streptavidin-DyLight™-594 or -488 conjugates (Jackson ImmunoResearch). Stained sections were mounted in Pro-Long Gold with DAPI (Invitrogen, Grand Island, NY, USA) and viewed using an Olympus BX60 fluorescence microscope. iVision software v. 4.0.0 (BioVision Technologies) was used for image collection.

Quantitative Real-Time Reverse-Transcriptase PCR (Q RT-PCR)

RNA was harvested as previously described (Richardson et al., 2006) from mid-exponential cultures ($OD_{660} = 0.5$) cultivated anaerobically in TSB lacking glucose and supplemented with 50 mM arginine. Alternatively, similarly grown cultures were supplemented with glucose (25mM) or cultured aerobically in its absence. Q RT-PCR was performed on 50 ng of total RNA using a My-iQ Thermocycler (BioRad, Indianapolis, IN) as previously described (Joshi et al., 2011).

Determination of Tissue Polyamine Content

TCA-soluble fractions of tissue homogenates (500 μg total protein equivalent) were neutralized with Na_2CO_3 and mixed with 200 μl fluorescamine (2 mg/ml in acetonitrile) combined with 150 μl Borate buffer (pH 8.0, 0.1M). The samples were incubated at room temperature for 10 min followed by chloroform extraction. The aqueous phase was washed with 6 ml of 15% MeOH on a Waters Sepak C-18 column, eluted with 1 ml of 100% MeOH and evaporated to 250 μl at 60° C. 100 μl of the eluate was combined with 150 μl H_2O and injected via Waters™ 717plus Autosampler into an Applied Biosystems 140B solvent delivery system and separated on a Waters SunFire™ C18 5 μm 2.1×150 mm column. Separation was achieved using a 0.1% TFA:MeOH gradient at 100 μl/min flow as follows: 15% MeOH for 4min then to 50% MeOH by 5 min. Gradient from 50% to 68% over 10 min, then to 70% in 1 minute. Finally, gradient from 70% to 100% in 10 minutes. Fluorescamine derivatized polyamines were detected via a Hewlett Packard 1046A programmable fluorescent detector (Ex = 405 nm, Em = 485 nm) and polyamine concentrations were quantified by comparing to known standards. Values were analyzed with a Peaksimple Chromatography Data System (SRI, Torrance, CA).

Flow Cytometry

Harvested tissues were strained through a 70 μm mesh filter then treated with type-1 collagenase and DNase (Worthington Biochem Corp., Lakewood, NJ). Cells were washed

then incubated with Fc Block (BD Biosciences). The antibodies used were anti-CD45-efluor 450 (eBiosciences, 30-f11), anit-CD11b-APC (eBio, M1/70), anti-GR1-PEcy7 (Biolegend, RB68C5), anti-CD3-FITC (BD Pharmagen, 145 2c11), anti-B220-FITC (BD, RA3-6B2), anti-iNOS-PE (Santa Cruz, polyclonal), sheep anti-Arginase-1 (R&D systems), and donkey anti-sheep-PE (R&D). Intracellular staining of iNOS and Arg-1 was performed as previously described (Neely et al., 2011). Live cells were scored using pacific orange conjugated succinimidyl ester. Data were collected using a FACS Cyan (Dako, Ft. Collins, CO) and analyzed using Summit software (Dako, Ft. Collins, CO). Graphs represent the percentage iNOS or Arginase-1 producing live cells that were CD45$^+$ CD11b$^+$, GR-1$^{Lo-Int,}$ and CD3$^-$, B220$^-$.

Supplementary Material

Refer to Web version on PubMed Central for supplementary material.

Acknowledgments

Literature Cited

Bartels MD, Hansen LH, Boye K, Sorensen SJ, Westh H. An unexpected location of the arginine catabolic mobile element (ACME) in a USA300-related MRSA strain. PLoS One. 2011; 6:e16193. [PubMed: 21283578]

Baydoun AR, Morgan DM. Inhibition of ornithine decarboxylase potentiates nitric oxide production in LPS-activated J774 cells. Br J Pharmacol. 1998; 125:1511–1516. [PubMed: 9884080]

Baze PE, Milano G, Verrando P, Renee N, Ortonne JP. Distribution of polyamines in human epidermis. Br J Dermatol. 1985; 112:393–396. [PubMed: 3994918]

Bubeck Wardenburg J, Bae T, Otto M, Deleo FR, Schneewind O. Poring over pores: alpha-hemolysin and Panton-Valentine leukocidin in Staphylococcus aureus pneumonia. Nat Med. 2007; 13:1405–1406. [PubMed: 18064027]

Bubeck Wardenburg J, Palazzolo-Ballance AM, Otto M, Schneewind O, DeLeo FR. Panton-Valentine leukocidin is not a virulence determinant in murine models of community-associated methicillin-resistant Staphylococcus aureus disease. The Journal of infectious diseases. 2008; 198:1166–1170. [PubMed: 18729780]

Chaturvedi R, Asim M, Lewis ND, Algood HM, Cover TL, Kim PY, Wilson KT. L-arginine availability regulates inducible nitric oxide synthase-dependent host defense against Helicobacter pylori. Infection and immunity. 2007; 75:4305–4315. [PubMed: 17562760]

Cohen, S. A Guide to the Polyamines. Oxford University Press; Oxford, UK: 2000.

Curran JN, Winter DC, Bouchier-Hayes D. Biological fate and clinical implications of arginine metabolism in tissue healing. Wound Repair Regen. 2006; 14:376–386. [PubMed: 16939563]

DeLeo FR, Otto M, Kreiswirth BN, Chambers HF. Community-associated meticillin-resistant Staphylococcus aureus. Lancet. 2010; 375:1557–1568. [PubMed: 20206987]

Di Meglio P, Perera GK, Nestle FO. The multitasking organ: recent insights into skin immune function. Immunity. 2011; 35:857–869. [PubMed: 22195743]

Diep BA, Gill SR, Chang RF, Phan TH, Chen JH, Davidson MG, Lin F, Lin J, Carleton HA, Mongodin EF, et al. Complete genome sequence of USA300, an epidemic clone of community-acquired meticillin-resistant Staphylococcus aureus. Lancet. 2006; 367:731–739. [PubMed: 16517273]

Diep BA, Stone GG, Basuino L, Graber CJ, Miller A, des Etages SA, Jones A, Palazzolo-Ballance AM, Perdreau-Remington F, Sensabaugh GF, et al. The arginine catabolic mobile element and

staphylococcal chromosomal cassette mec linkage: convergence of virulence and resistance in the USA300 clone of methicillin-resistant Staphylococcus aureus. J Infect Dis. 2008; 197:1523–1530. [PubMed: 18700257]

Ellington MJ, Yearwood L, Ganner M, East C, Kearns AM. Distribution of the ACME-arcA gene among methicillin-resistant Staphylococcus aureus from England and Wales. J Antimicrob Chemother. 2008; 61:73–77. [PubMed: 17989100]

Fuller JR, Vitko NP, Perkowski EF, Scott E, Khatri D, Spontak JS, Thurlow LR, Richardson AR. Identification of a lactate-quinone oxidoreductase in Staphylococcus aureus that is essential for virulence. Frontiers in Cellular and Infection Microbiology. 2011; 1

Gantwerker EA, Hom DB. Skin: histology and physiology of wound healing. Clin Plast Surg. 2012; 39:85–97. [PubMed: 22099852]

Goering RV, McDougal LK, Fosheim GE, Bonnstetter KK, Wolter DJ, Tenover FC. Epidemiologic distribution of the arginine catabolic mobile element among selected methicillin-resistant and methicillin-susceptible Staphylococcus aureus isolates. J Clin Microbiol. 2007; 45:1981–1984. [PubMed: 17409207]

Harvey CJ, LeBouf RF, Stefaniak AB. Formulation and stability of a novel artificial human sweat under conditions of storage and use. Toxicol In Vitro. 2010; 24:1790–1796. [PubMed: 20599493]

Hochgrafe F, Wolf C, Fuchs S, Liebeke M, Lalk M, Engelmann S, Hecker M. Nitric oxide stress induces different responses but mediates comparable protein thiol protection in Bacillus subtilis and Staphylococcus aureus. J Bacteriol. 2008; 190:4997–5008. [PubMed: 18487332]

Joshi GS, Spontak JS, Klapper DG, Richardson AR. Arginine catabolic mobile element encoded speG abrogates the unique hypersensitivity of Staphylococcus aureus to exogenous polyamines. Mol Microbiol. 2011; 82:9–20. [PubMed: 21902734]

Kobayashi SD, Malachowa N, Whitney AR, Braughton KR, Gardner DJ, Long D, Bubeck Wardenburg J, Schneewind O, Otto M, Deleo FR. Comparative analysis of USA300 virulence determinants in a rabbit model of skin and soft tissue infection. The Journal of infectious diseases. 2011; 204:937–941. [PubMed: 21849291]

Li M, Cheung GY, Hu J, Wang D, Joo HS, Deleo FR, Otto M. Comparative analysis of virulence and toxin expression of global community-associated methicillin-resistant Staphylococcus aureus strains. The Journal of infectious diseases. 2010; 202:1866–1876. [PubMed: 21050125]

Li M, Diep BA, Villaruz AE, Braughton KR, Jiang X, DeLeo FR, Chambers HF, Lu Y, Otto M. Evolution of virulence in epidemic community-associated methicillin-resistant Staphylococcus aureus. Proc Natl Acad Sci U S A. 2009; 106:5883–5888. [PubMed: 19293374]

Lipinska U, Hermans K, Meulemans L, Dumitrescu O, Badiou C, Duchateau L, Haesebrouck F, Etienne J, Lina G. Panton-Valentine leukocidin does play a role in the early stage of Staphylococcus aureus skin infections: a rabbit model. PLoS One. 2011; 6:e22864. [PubMed: 21850240]

Loffler B, Hussain M, Grundmeier M, Bruck M, Holzinger D, Varga G, Roth J, Kahl BC, Proctor RA, Peters G. Staphylococcus aureus panton-valentine leukocidin is a very potent cytotoxic factor for human neutrophils. PLoS Pathog. 2010; 6:e1000715. [PubMed: 20072612]

Makhlin J, Kofman T, Borovok I, Kohler C, Engelmann S, Cohen G, Aharonowitz Y. Staphylococcus aureus ArcR controls expression of the arginine deiminase operon. J Bacteriol. 2007; 189:5976–5986. [PubMed: 17557828]

McDougal LK, Steward CD, Killgore GE, Chaitram JM, McAllister SK, Tenover FC. Pulsed-field gel electrophoresis typing of oxacillin-resistant Staphylococcus aureus isolates from the United States: establishing a national database. J Clin Microbiol. 2003; 41:5113–5120. [PubMed: 14605147]

Miko BA, Uhlemann AC, Gelman A, Lee CJ, Hafer CA, Sullivan SB, Shi Q, Miller M, Zenilman J, Lowy FD. High prevalence of colonization with Staphylococcus aureus clone USA300 at multiple body sites among sexually transmitted diseases clinic patients: an unrecognized reservoir. Microbes Infect. 2012

Miller LS, Cho JS. Immunity against Staphylococcus aureus cutaneous infections. Nat Rev Immunol. 2011; 11:505–518. [PubMed: 21720387]

Miragaia M, de Lencastre H, Perdreau-Remington F, Chambers HF, Higashi J, Sullam PM, Lin J, Wong KI, King KA, Otto M, et al. Genetic diversity of arginine catabolic mobile element in Staphylococcus epidermidis. PLoS One. 2009; 4:e7722. [PubMed: 19893740]

Montgomery CP, Boyle-Vavra S, Adem PV, Lee JC, Husain AN, Clasen J, Daum RS. Comparison of virulence in community-associated methicillin-resistant Staphylococcus aureus pulsotypes USA300 and USA400 in a rat model of pneumonia. The Journal of infectious diseases. 2008; 198:561–570. [PubMed: 18598194]

Montgomery CP, Boyle-Vavra S, Daum RS. The arginine catabolic mobile element is not associated with enhanced virulence in experimental invasive disease caused by the community-associated methicillin-resistant Staphylococcus aureus USA300 genetic background. Infect Immun. 2009; 77:2650–2656. [PubMed: 19380473]

Montgomery CP, Boyle-Vavra S, Daum RS. Importance of the global regulators Agr and SaeRS in the pathogenesis of CA-MRSA USA300 infection. PLoS One. 2010; 5:e15177. [PubMed: 21151999]

Neely CJ, Maile R, Wang MJ, Vadlamudi S, Meyer AA, Cairns BA. Th17 (IFNgamma− IL17+) CD4+ T cells generated after burn injury may be a novel cellular mechanism for postburn immunosuppression. J Trauma. 2011; 70:681–690. [PubMed: 21610359]

Popovich KJ, Weinstein RA, Hota B. Are community-associated methicillin-resistant Staphylococcus aureus (MRSA) strains replacing traditional nosocomial MRSA strains? Clin Infect Dis. 2008; 46:787–794. [PubMed: 18266611]

Reyes J, Rincon S, Diaz L, Panesso D, Contreras GA, Zurita J, Carrillo C, Rizzi A, Guzman M, Adachi J, et al. Dissemination of methicillin-resistant Staphylococcus aureus USA300 sequence type 8 lineage in Latin America. Clin Infect Dis. 2009; 49:1861–1867. [PubMed: 19911971]

Richardson AR, Dunman PM, Fang FC. The nitrosative stress response of Staphylococcus aureus is required for resistance to innate immunity. Mol Microbiol. 2006; 61:927–939. [PubMed: 16859493]

Richardson AR, Libby SJ, Fang FC. A nitric oxide-inducible lactate dehydrogenase enables Staphylococcus aureus to resist innate immunity. Science. 2008; 319:1672–1676. [PubMed: 18356528]

Satriano J. Arginine pathways and the inflammatory response: interregulation of nitric oxide and polyamines: review article. Amino Acids. 2004; 26:321–329. [PubMed: 15290337]

Schechter-Perkins EM, Mitchell PM, Murray KA, Rubin-Smith JE, Weir S, Gupta K. Prevalence and predictors of nasal and extranasal staphylococcal colonization in patients presenting to the emergency department. Ann Emerg Med. 2011; 57:492–499. [PubMed: 21239081]

Shore AC, Rossney AS, Brennan OM, Kinnevey PM, Humphreys H, Sullivan DJ, Goering RV, Ehricht R, Monecke S, Coleman DC. Characterization of a novel arginine catabolic mobile element (ACME) and staphylococcal chromosomal cassette mec composite island with significant homology to Staphylococcus epidermidis ACME type II in methicillin-resistant Staphylococcus aureus genotype ST22-MRSA-IV. Antimicrob Agents Chemother. 2011; 55:1896–1905. [PubMed: 21343442]

Sun JL, Zhang SK, Chen JY, Han BZ. Metabolic profiling of Staphylococcus aureus cultivated under aerobic and anaerobic conditions with (1)H NMR-based nontargeted analysis. Can J Microbiol. 2012

Sunkara PS, Rosenberger AL. Antimetastatic activity of DL-alpha-difluoromethylornithine, an inhibitor of polyamine biosynthesis, in mice. Cancer Res. 1987; 47:933–935. [PubMed: 3100031]

Talan DA, Krishnadasan A, Gorwitz RJ, Fosheim GE, Limbago B, Albrecht V, Moran GJ. Comparison of Staphylococcus aureus from skin and soft-tissue infections in US emergency department patients, 2004 and 2008. Clin Infect Dis. 2011; 53:144–149. [PubMed: 21690621]

Thurlow LR, Hanke ML, Fritz T, Angle A, Aldrich A, Williams SH, Engebretsen IL, Bayles KW, Horswill AR, Kielian T. Staphylococcus aureus biofilms prevent macrophage phagocytosis and attenuate inflammation in vivo. J Immunol. 2011; 186:6585–6596. [PubMed: 21525381]

Thurlow LR, Joshi GS, Richardson AR. Virulence Strategies of the Dominant USA300 Lineage of Community Associated Methicillin Resistant Staphylococcus aureus (CA-MRSA). FEMS Immunol Med Microbiol. 2012

Urushibara N, Kawaguchiya M, Kobayashi N. Two novel arginine catabolic mobile elements and staphylococcal chromosome cassette mec composite islands in community-acquired methicillin-resistant Staphylococcus aureus genotypes ST5-MRSA-V and ST5-MRSA-II. J Antimicrob Chemother. 2012; 67:1828–1834. [PubMed: 22563013]

Zhang M, Wang H, Tracey KJ. Regulation of macrophage activation and inflammation by spermine: a new chapter in an old story. Crit Care Med. 2000; 28:N60–66. [PubMed: 10807317]

HIGHLIGHTS

- USA300 ACME Arginine-deiminase system (ARC) allows *S.aureus* growth in acidic environments

- ACME-Arc drives excess host polyamine synthesis, which is toxic to *S. aureus*

- ACME-encoded polyamine-resistance enzyme SpeG is essential for combating excess polyamines

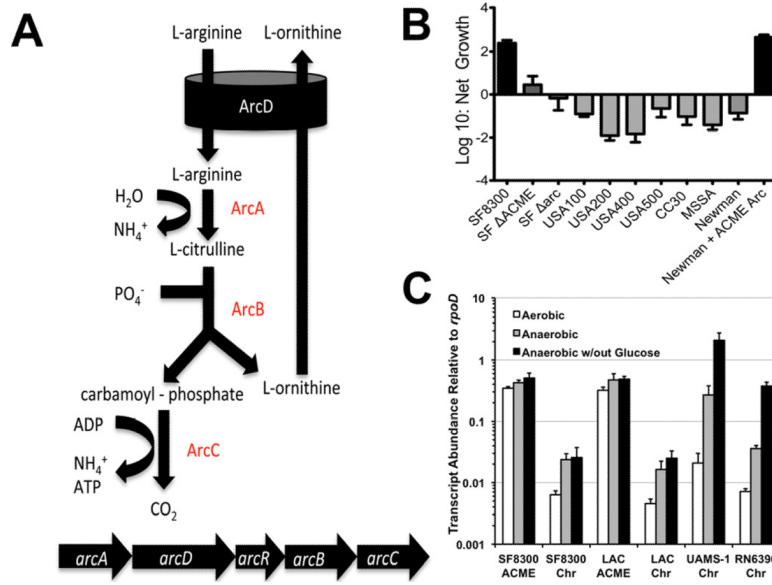- Inhibiting host polyamine production restores Δ*speG* persistence and affects wound healing

Figure 1. Constitutive USA300 ACME-Arc provides resistance to skin-like acidity
A. Arc system of *S. aureus* converts extracellular arginine to ornithine while producing ATP and ammonia. **B**. Growth of ACME-postive and –negative (grey bars) *S. aureus* in defined media replete with arginine and acidified (pH 5.0) with lactic acid. See also (Figure S1). **C**. Quantitative RT-PCR showing constitutive expression of ACME-*arcA* relative to chromosomal-*arcA*.
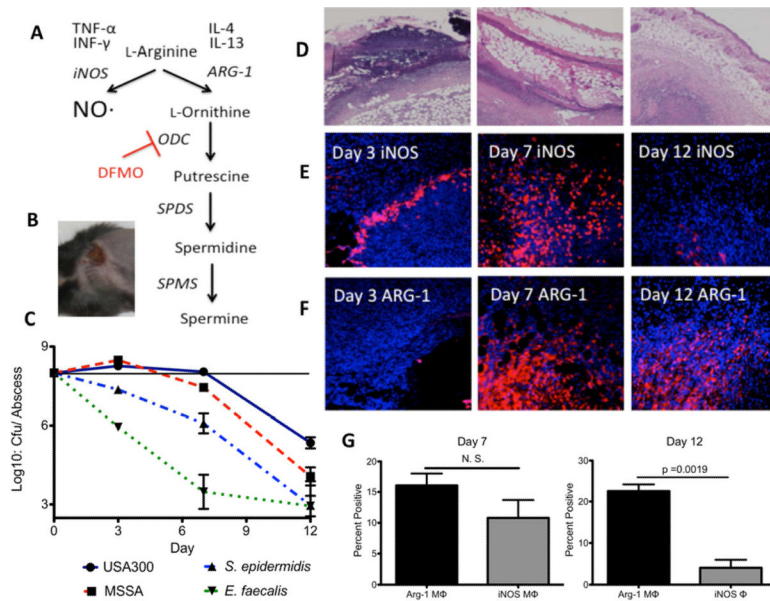
Figure 2. The fate of host arginine during USA300 *S. aureus* skin infections
A. Arginine metabolism in response to cytokines during skin infections. **B**. Dermonecrotic lesion 3 days after subcutaneous inoculation with 1×10^8 cfu of USA300 *S. aureus*. **C**. Viable cfu/abscess over time from mice infected with WT USA300 *S. aureus*, Methicillin-sensitive *S. aureus* Newman (MSSA), *S. epidermidis* RP62a or *E. faecalis* V583. *S. epidermidis* and *E. faecalis* abscesses harbored significantly fewer viable cfu compared with USA300 at all three timepoints whereas *S. aureus* strain Newman was significantly attenuated compared with USA300 at days 7 and 12 (p 0.05 Mann-Whitney). **D**. Representative H&E stained tissue imaged at 4× magnification from an infected lesion 3, 7 and 12 dpi. **E**. Immunofluorescent staining of tissue imaged at 20× from an infected lesion 3, 7 and 12 dpi using α-iNOS antibodies and counterstained with DAPI. **F**. Similar to Figure 1E except using α-Arg-1 primary antibodies. **G**. Results of flow cytometery on extracted abscess tissue from day 7 and 12 murine SSTIs. Cells were gated on the living macrophage-like cell population (CD45^{Hi} CD11b^{Hi} GR-1^{Lo-Int} CD3^{Lo} B220^{Lo}) and counted for intracellular staining with either anti-Arg-1 or anti-iNOS antibodies.
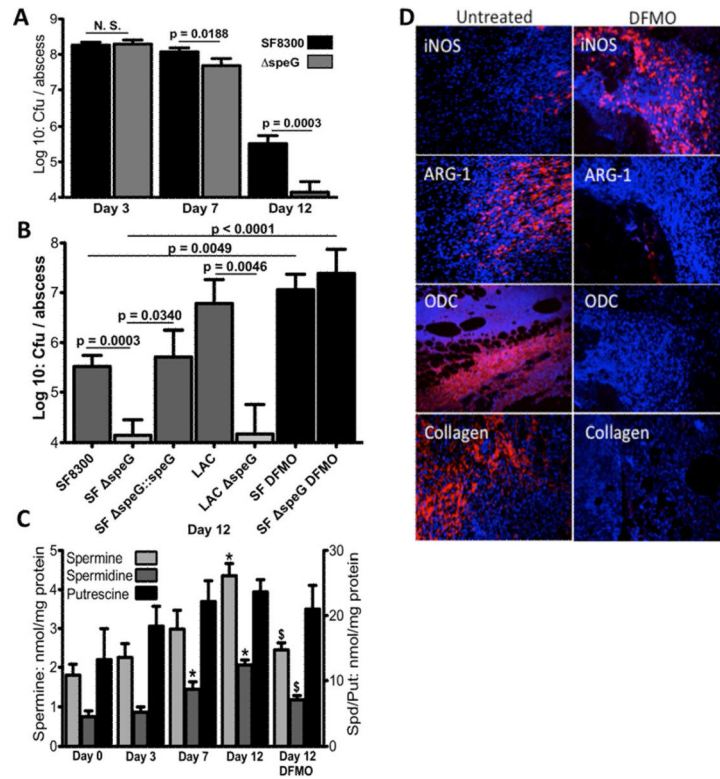
Figure 3. USA300 polyamine-resistance is essential for persistence during the post-inflammatory wound healing response

A. Viable cfu per abscess of WT USA300 and isogenic Δ*speG* at 3, 7 and 12 dpi. Significance was assessed via Mann-Whitney. **B**. Viability of WT USA300 clones (SF8300 (SF) and LAC) and isogenic Δ*speG* mutants in 12-day abscesses. Repaired Δ*speG* (SF Δ*speG::speG*) is fully virulent. DFMO treatment abrogates Δ*speG* attenuation. **C**. Increasing polyamine levels (nmol/mg tissue) detected in *S. aureus* abscesses throughout the infection. (*) significantly higher levels compared with day 0. ($) significantly reduced levels in tissue from DFMO treated animals (p< 0.05 Man-Whitney). **D**. Immunofluorescent staining of day 12 abscesses imaged at 20× magnification from mice treated with/without DFMO using indicated antibodies and counterstained with DAPI.
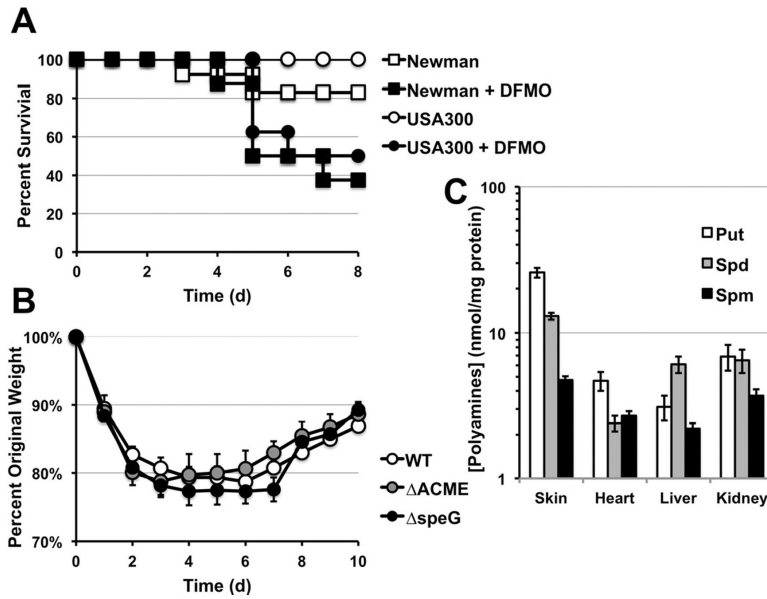
Figure 4. Polyamines are critical during sepsis, but levels are not sufficient to directly kill *S. aureus*

A. Survival of eight 4–6 week female C57BL/6 mice (treated or untreated with DFMO) following *i.v.* inoculation with 5×10^6 cfu of USA300 *S. aureus* or MSSA strain Newman. DFMO treatment significantly exacerbated disease outcomes for both USA300 and Newman infections ($p < 0.05$, Kaplan Meier). **B**. Weight loss following *i.v.* inoculation of 8 mice with 5×10^6 cfu of WT USA300 and isogenic ΔACME or Δ*speG* mutants. **C**. Organ tissue polyamines levels detected 7 days after infection when mice begin to resume weight gain compared with levels found in resolving *S. aureus* abscesses.